

Diffraction Analysis of Graphene Starsmoke
Nathan Hunton
University of Missouri in St. Louis
Professor Phil Fraundorf, advisor

Cores of micron-sized graphite spheres from AGB star atmospheres contain our first naturally-occurring samples of solid unlayered-graphene, and may be characteristic of much condensed carbon in the interstellar medium. Diffraction profiles provide structural constraints on their formation process, e.g. with possible evidence for a combination of superstructure and gap-filling sheets.

I. Introduction

Here we discuss the results of a project in which we're attempting to determine the sizes of a particular class of flat molecules by means of electron diffraction analysis. These molecules are located in the cores of micron-sized graphitic spheres recovered from a meteorite that struck southeastern Australia in 1987¹. Isotopic data tells us that most of these spheres were condensed in the atmosphere of asymptotic giant branch stars^{2,3}. This core material is of interest for three reasons: A) It provides laboratory information on processes in cool stellar atmospheres. B) The molecular structure of these cores may be shared by a significant fraction of the condensed carbon in the interstellar medium, and hence be part of the history of our own carbon atoms as well. C) Processes that create unlayered graphene, including single-walled carbon nanotubes and nanohorns, are of intense interest in modern materials physics because of their present and future applications in electronics, composite materials, and the growing range of areas impacted by nanotechnology⁴.

II. Observations

II.A Experimental Data

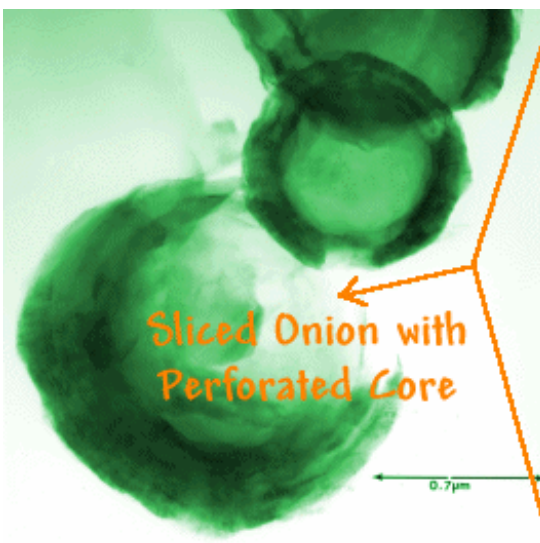


Figure 1: Brightfield transmission electron microscope (TEM) image of presolar graphite onions with dark rims and unlayered graphene cores, after sectioning and deposition on a holey carbon film. The perforated core region is an excellent location for high resolution imaging.

A brightfield transmitted electron image of several of these spheres, which we refer to as “onions” because each has many outer “skins”, is shown in Figure 1. What are these strange-looking objects made of? Electron diffraction profiles from the outer shells of the onions [Fig 2 left] identify the rims as graphitic layers wrapped onion-style around the grain. Diffraction profiles of core material, while indicating carbon, lack all diffraction peaks associated with graphitic layering [Fig 2 right]. This means that the core is graphene—unlayered graphite. The evidence, as uncovered by means of diffraction¹ and high-resolution transmission electron microscope^{5,6} images [see the atom-thick cones viewed edge-on in Fig 3], suggests that the material in the core consists of many tiny sheets of graphene, some of which have been warped into broad cones by a single pentagonal defect.

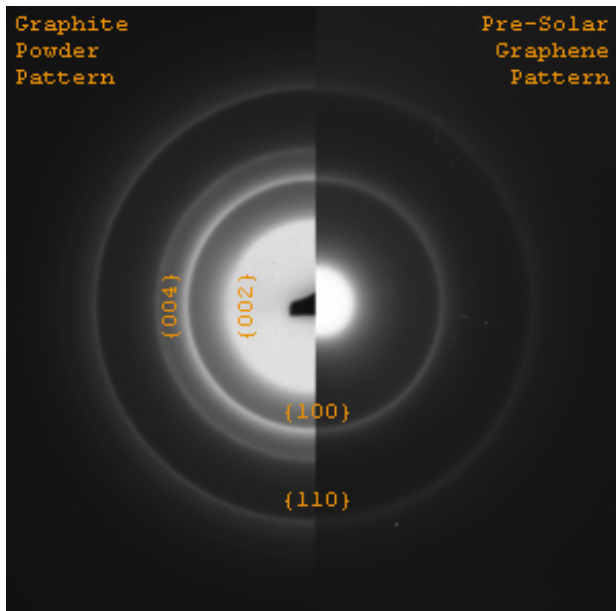


Figure 2: Electron powder diffraction patterns - left half is terrestrial pyrolytic graphite; right half is graphene from the core of a presolar onion. Note the presence of only $\{hk0\}$ spacings in the latter, showing an absence of graphite layering.

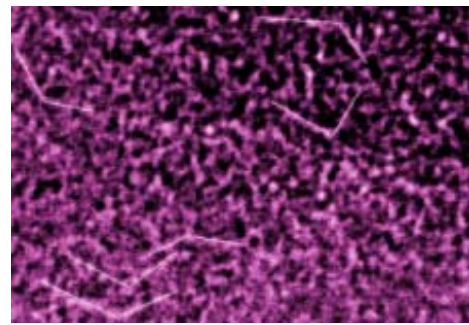


Figure 3: Negative of a high resolution TEM image, in which several likely edge-on nanocones have been marked⁶. Field width is about 18 nm.

Over the past year, our analysis of the diffraction profiles has focused on determining the size distribution (more technically the distribution of coherence widths) of these graphene sheets. A Philips 430 transmission electron microscope (TEM) was used to record images and electron powder diffraction patterns of the onions and their cores. The patterns were converted to profiles of intensity as a function of distance from the center, with a domain of the set of real numbers from 0 to 255 (in some cases 0 to 65,536) in arbitrary units. These profiles were analyzed by removing the background and measuring certain attributes of the resulting peaks. Fig 4 illustrates the creation of a background-subtracted profile from each of two different interstellar onion core diffraction patterns. All scales are linear.

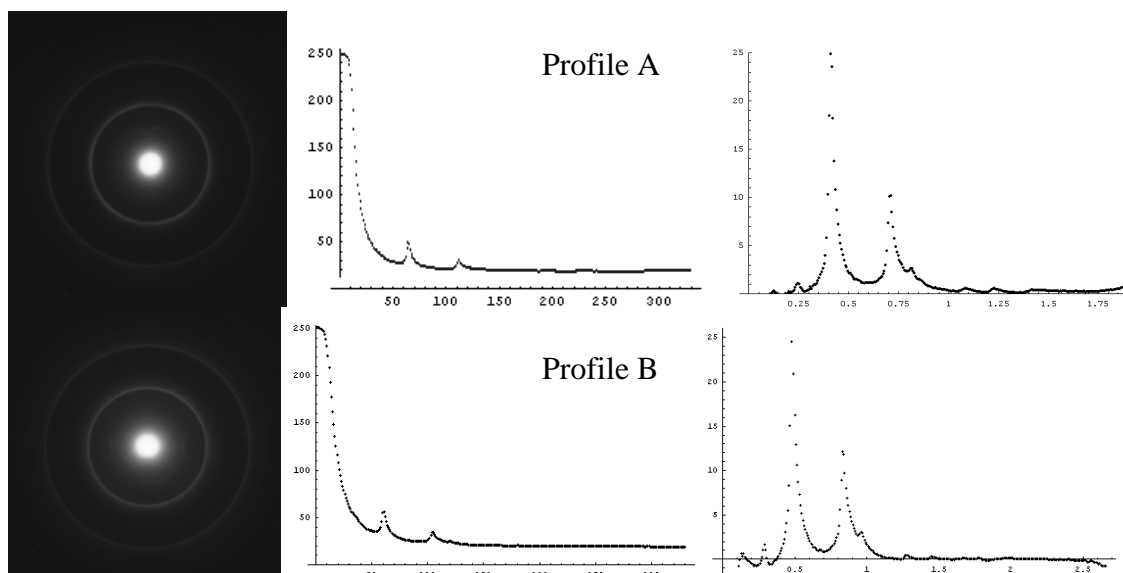


Figure 4: Data from two different onions. Diffraction patterns are on the left, azimuthal average profiles in the center, and background-subtracted profiles (with slightly different horizontal scales) showing diffraction peaks to the right. The two main peaks correspond to graphene (100) and (110) spacings.

Recording a diffraction pattern is different from taking a snapshot with a regular camera. Where the photographic camera usually exposes its film to incoming light for less than a second, the film used to record electron diffraction patterns is often left exposed to electrons for ten to fifty seconds. One may therefore wonder about the effect of time on the recorded intensities. Could the exposure time affect the peak shapes, and if so how? To answer this question, we recorded the diffraction pattern of the same onion on numbered negatives at three different exposure periods: ten, twenty, and fifty seconds (negatives 3180, 3181, and 3179 respectively). The resulting patterns from the same core are seen in Figure 5.

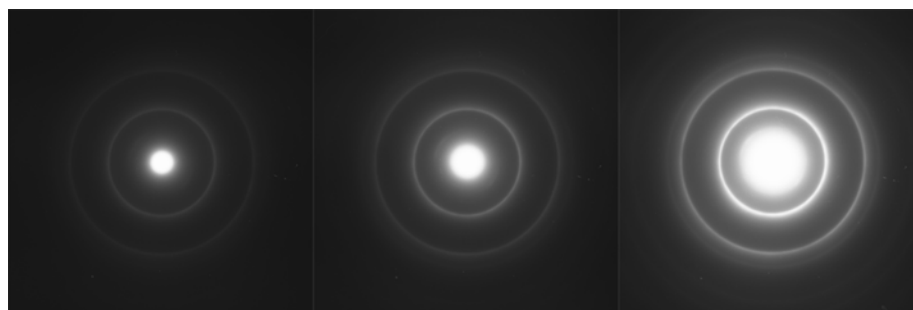


Figure 5: From left to right: film negatives 3180 (10 s), 3181 (20 s), and 3179 (50 s).

Each pattern has the same set of rings, but differs in the brightness of the rings and the size of the center spot. By plotting the grey value of each point in the 2nd and 3rd images versus the grey value in the first, the remarkable pattern in Fig. 6 emerges. This confirms that in unsaturated films digitized under the same scanner gain settings, the value of the intensity recorded at any particular point is directly proportional to time and hence to electron intensity.

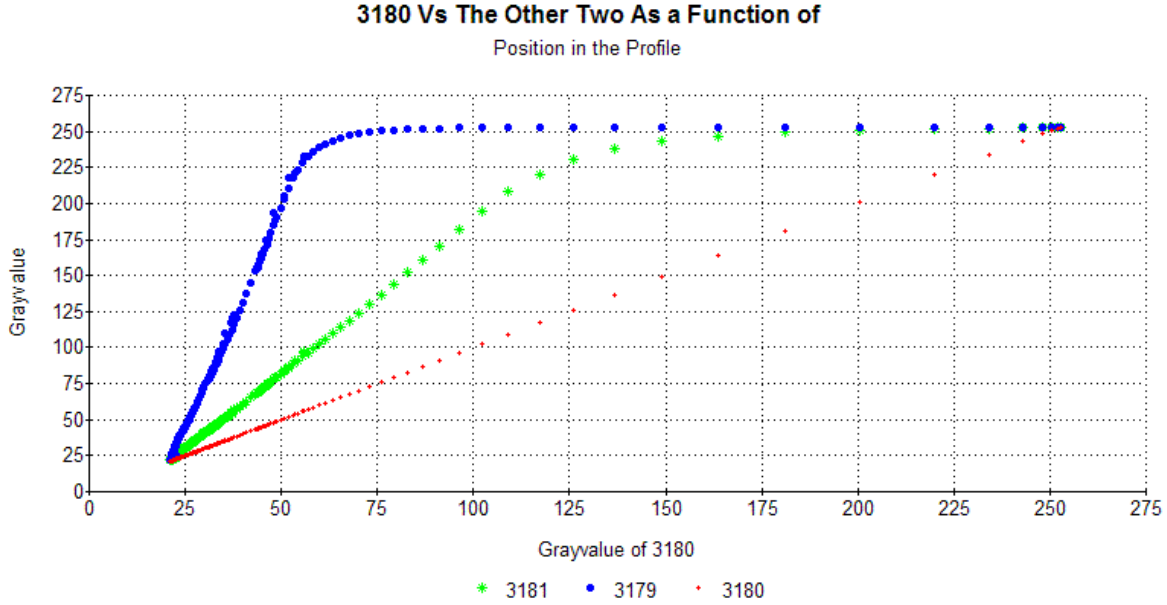


Fig 6: Taking ≈ 23 as a background noise version of zero, the ratio of grayvalues at a given x on any pair of profiles roughly equals the corresponding ratio of exposure times until one of the gray values passes $y \approx 200$ (which represents overexposure of the film). See the values that fall on the $x = 50$ line for an example.

II.B Diffraction profile models

Each experimental diffraction pattern was approximated with two functions. The first function (first three terms in the equation below) was usually a second-order inverse equation to account for the unwanted “background noise”. The second function was the peak model itself, in this case shown to result from sheets distributed similarly in two distinct size ranges. Thus the resulting fit equation often took the form

$$y[x] = c_1 + \frac{c_2}{x} + \frac{c_3}{x^2} + c_4 I[x, w_1, \sigma_1] + c_5 I[x, w_2, \sigma_2] .$$

Here the c_i are fitting parameters, and the function $I[x, w, \sigma]$ represents a model profile for electron diffraction from randomly-oriented (and for example log-normally distributed) graphene sheets of mean size w and size standard deviation σ .

For the peak models themselves, we began with a model for electron scattering as a function of angle or spatial frequency x from a grating with periodicity d and sheet width w as projected in the incident wave direction. Basically one expects a diffraction spot of width $1/w$ centered at $x = 1/d$. In Gaussian approximation, the intensity G as a function of spatial frequency x looks something like...

$$G\left[x, \frac{1}{d}, \frac{1}{w}\right] = \frac{1}{\sqrt{2\pi} * \frac{1}{w}} * e^{-\frac{(x - \frac{1}{d})^2}{2 * (\frac{1}{w})^2}}$$

Averaging this over all orientations gives a peak shape with the high-frequency tail characteristic of atom-thick sheets⁷ and a peak width inversely proportional to w . The equation for this averaging process may be written...

$$P[x, d, w] = \frac{1}{2\pi} * \int_0^{2\pi} (1) d\phi \int_0^{\pi/2} (G[x, \frac{1}{d * \sin \theta}, \frac{1}{w * \sin \theta}] * \sin \theta) d\theta.$$

Before adding together such profiles from the periodicities found in a graphene lattice, in some cases we further combined the scattering from a mix of sheet sizes that were log-normally distributed with mean w and standard deviation σ . This log-normal probability distribution can be written

$$p[x, w, \sigma] = \frac{e^{-\left(\ln x - \ln \frac{w}{\sqrt{1 + (\sigma/w)^2}}\right)^2 / 2 * \ln[1 + (\sigma/w)^2]}}{x \sqrt{2\pi \ln[1 + (\sigma/w)^2]}}.$$

Normal distributions are widespread in nature, but regular normal distributions have as their domain all real numbers. Since we certainly had no particles of diameter less than or equal to zero, log-normal distributions—the domains of which are only defined over the set of positive reals—were used.

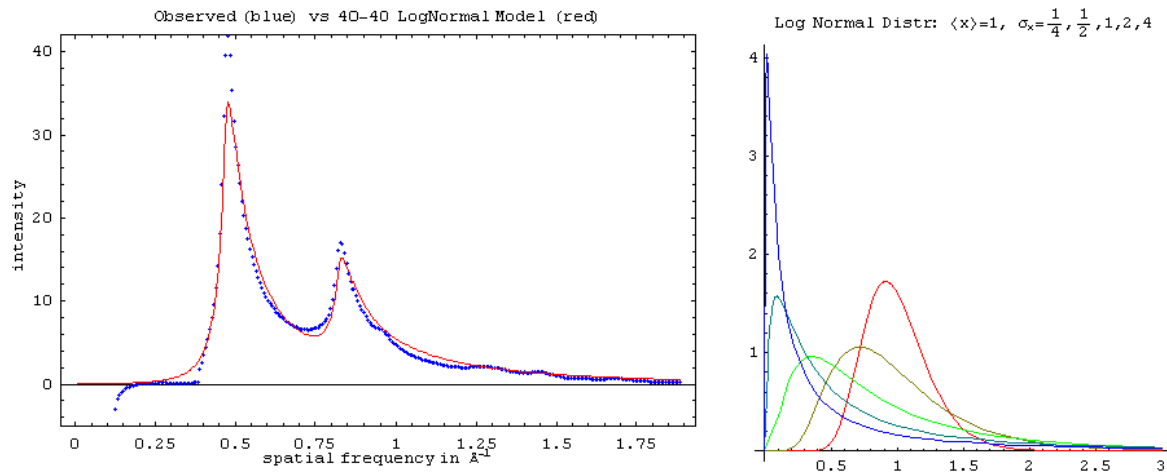


Figure 7: Left: Log-normal model (red line) superimposed on experimental data (blue dots); Right: Log-normal distributions of mean value 1 and standard deviations from 1/4 (red) to 4 (blue).

The peak-fitting algorithms that use the above functions (illustrated in Fig. 7) are often slow. However, these functions are useful not only for analyzing experimental data but also for generating theoretical data that can be studied, a process that takes much less time than fitting data.

III. Data Analysis

In this section, we discuss observations based on the models described above to illustrate how quantitative electron diffraction studies can provide information on the distribution of graphene sheets in these specimens.

III.A Shortcomings of a single size distribution peak

We describe with help from Figure 7 several features characteristic of modeled diffraction profiles (in particular those modeling sheets of a single size and those modeling sheets of a size range described by a normal distribution) as they compare to the experimental profiles. The first trait is that, when the theoretical peak is scaled in the vertical direction to make its tails (or “wings”) fit those of the experimental peak, the experimental peak is too narrow at the top. This is apparent in the figure even though background subtraction in this case actually cut off more of the first experimental wing on the left side than is reasonable (note the abrupt onset of the first experimental peak at $x = 0.38$). Assuming the mean of the log-normal sheet size distribution to be 60 Angstroms instead of 40 yields a better fit to the peak top at the cost of unacceptably small wings. Moreover increasing the standard deviation of the log-normal distribution fails to correct this problem, i.e. the peak width at the top grows too rapidly, relative to the wing broadening, to provide a good fit. All of this suggests that two different distributions of graphene sheet sizes may be required to explain the experimental data, at least in context of models described above.

Another problem with a single-peaked size distribution using these models is the cusp between the two peaks (note the rightward dip in line below the dots near $x = .8$ in Fig. 7). We are now testing to see if replacing the Gaussian approximation in section II.B above with a sinc scattering model will correct this difficulty. If not, we will thus have two reasons for considering the inclusion of a second peak in the sheet size distribution.

III.B Two-peak models

Assuming that single-peak models are not adequate to explain experimental diffraction profiles from interstellar graphite onion cores, it is likely that sheets with average size around 60 Angstroms, combined with a broader distribution of sheet sizes in the 10 to 20 Angstrom size range, will fit experimental profiles nicely. That's because smaller "gap-filling" sheets would allow one to adjust diffraction peak wings independently of peak sharpness, as determined by the size of larger "superstructure" sheets. *Mathematica* routines to automate calculation of optimum fits in reasonable times are being prepared, as model refinement continues.

IV. Discussion and Summary

In the quest for novel nano-materials to be used in industry, medicine, computation, and manufacturing, these specimens may represent the first^{6,8} unlayered-graphene solids found to

occur in nature. Understanding their molecular make-up, formation process, and journey here may thus be of importance in material science, as well as to our understanding of carbon's place in our universe⁹. Questions in the latter context are, for example: How much of the condensed carbon in the interstellar medium is in this form¹⁰, and did such carbon play an important part in the early days of our solar system?

We have reported here laboratory work on the structure of this core material which indicates that electron diffraction can put constraints on the distribution of molecule sizes. We hope to use these constraints, in combination with aberration-corrected sub-Angstrom TEM images of this material, to constrain possible formation models in the future. Formation models under consideration to explain their unusual structure include, but are not limited to: (i) accretion of polycyclic aromatic hydrocarbon molecules¹, (ii) atom by atom condensation in the presence of high radiation fluxes, and (iii) solidification from liquid carbon droplets¹¹. With luck this work can proceed in concert with astrophysical studies of red giant atmospheres and of the interstellar medium, as well as laboratory synthesis of novel carbon phases.

V. References

- ¹Bernatowicz, Thomas J., Ramanath Cowsik, Patrick C. Gibbons, Katharina Lodders, et. al. 1996. Constraints on Stellar Grain Formation from Presolar Graphite in the Murchison Meteorite. The Astrophysical Journal, 472:760-782.
- ²Zinner, E., S. Amari, B. Wopenka, and R.S. Lewis. 1995. Interstellar Graphite in Meteorites: Isotopic Compositions And Structural Properties of Single Graphite Grains from Murchison. Meteoritics, 30:209-26.
- ³Bernatowicz, Thomas J., and Robert M. Walker. 1997. Ancient Stardust in the Laboratory. Physics Today, December, 26-32.
- ⁴Rawstern, Rocky. 2003. Nanotechnology Surveys April 2003. <http://nanotech-now.com/nanotube-survey-april2003.htm>
- ⁵Fraundorf, P., K. Brewer, D. Dawkins, M. Truong, and D. Witt. 2000. The Core-rim Structure of Pre-solar Graphite Onions. Meteoritics and Planetary Science, 35(5):A56-57.
- ⁶Fraundorf, P. and M. Wackenhut. 2002. The core structure of pre-solar graphite onions. Astrophysical Journal Letters, 578(2): L153-L156.
- ⁷Warren, B.E. 1941. X-ray Diffraction in Random Layer Lattices. Phys. Rev., 59(9):693-698.
- ⁸Jaszczak, John A., George W. Robinson, Svetlana Dimovski, and Yury Gogotsi. Naturally Occurring Graphite Cones. Carbon, 2003.
- ⁹Amari, S., R.S. Lewis, and E. Anders. 1994. Interstellar Grains in Meteorites: I. Isolation of SiC, Graphite, and Diamond; Size Distributions of SiC and Graphite. Geochimica et Cosmochimica Acta, 58:459-70.
- ¹⁰Draine, B.T. and Sangeeta Malhotra. 1993 September 10. On Graphite and the 2175 Angstrom Extinction Profile. The Astrophysical Journal, 414:632-645.
- ¹¹Kasuya, D., M. Yudasaka, K. Takahashi, F. Kokai, and S. Iijima. 2002. J. Phys. Chem. B, 106:4947-4951.